iScience, Volume *23*

Supplemental Information

A Non-genetic Mechanism Involving the Integrin β4/Paxillin Axis Contributes to Chemoresistance in Lung Cancer

Atish Mohanty, Arin Nam, Alex Pozhitkov, Lu Yang, Saumya Srivastava, Anusha Nathan, Xiwei Wu, Isa Mambetsariev, Michael Nelson, A.R. Subbalakshmi, Linlin Guo, Mohd W. Nasser, Surinder K. Batra, John Orban, Mohit Kumar Jolly, Erminia Massarelli, Prakash Kulkarni, and Ravi Salgia

Supplemental Table and Figure Legends

Table S1. **Genes upregulated in cisplatin-resistant lung adenocarcinoma cell line from Molecular Signatures Database (MSigDB), Broad Institute.** Related to Figure 1.

Table S2. **Cox proportional hazards model: Survival ~ Sex + Stage + Age + PXN * ITGB4.** Related to Figure 1F.

Table S3. DAVID analysis of 96 unique genes downregulated in double knockdown of PXN and ITGB4. Related to Figure 5D-F.

Table S4. DAVID analysis of 206 common genes downregulated in single and double knockdown of PXN and ITGB4. Related to Figure 5D-F.

Table S5. **MiRNAs differentially regulated by single and double knockdown of PXN and ITGB4.** Related to Figure 8B-D.

Table S6. **SiRNA sequences used for knockdown experiments.** Related to Figures 2-7.

Figure S1. Expression of ITGA6 in NSCLC cell lines. Related to Figure 1B.
Protein expression of ITGA6 and PXN in the 5 KRAS mutant and 5 KRAS WT NSCLC cell lines. SW480 cells were used as positive control for ITGA6 expression.

Figure S2. Variability of expression of PXN and ITGB4 in tumor tissue samples. Related to Figure 1G.
A) Immunohistochemistry staining of lung adenocarcinoma tumor tissue showed that Case 1 had high PXN and intermediate ITGB4 expression. In Case 2, PXN expression is low and ITGB4 expression is high. In Case 3, both PXN and ITGB4 expression are low. **B)** and **C)** Multiplex staining of ITGB4 and PXN staining in 5 City of Hope patients. The images were deconvoluted using QuPath software, and percentage of area was calculated for either ITGB4 or PXN or both. Data are represented as mean +/- SD.

Figure S3. ITGB4 knockdown attenuates cell proliferation in commonly used NSCLC cell lines. Related to Figure 2.
A) Stable cell lines were generated to express nuclear mKate2 red fluorescent protein (RFP) using the NucLight Red Lentivirus Reagent (Essen BioScience). Upon selection with puromycin, cells were analyzed with the IncuCyte software to create a mask around each individual nucleus and obtain accurate real-time cell counts for proliferation assays. **B)** Effect of 3 different ITGB4 siRNA constructs (A, B, C) on cell proliferation over the course of 72 h in H358 cells. **C)** Effect of 3 different ITGB4 siRNA constructs (A, B, C) on cell proliferation over the course of 72 h in A549 cells. **D)** Immunoblot confirming ITGB4 knockdown upon Si ITGB4 transfection in H358 and A549 cells. Data are represented as mean +/- SD. (****p<0.0001)

Figure S4. ITGB4 knockdown has a specific effect in NSCLC compared to other integrin forms. Related to Figure 2.
A) Doubling times for H2009 and H1993 cells transfected with scramble siRNA (siControl) were measured and compared to that of cells with ITGB4 knockdown (siITGB4). **B)** H2009 cells transfected with 10 nM of siRNA constructs A, B, and C, targeting ITGA7 had minimal effect on proliferation. **C)** Knocking down ITGB4 increased mRNA expression of other integrin beta forms such as ITGB1, ITGB2, and ITGB3 but had no significant effect on the expression of ITGA7. **D)** In order to nullify the effect of ITGB3 rescue, H2009 cells transfected with siRNA ITGB4 were treated with ITGB3 inhibitors. There was no significant effect in the fold change in proliferation compared to the ITGB4 knockdown cells. **E)** Scratch wound healing assays were performed by creating an initial scratch wound with the WoundMaker tool. Wound closure was quantitated by monitoring cells that migrated to fill the initial wound. Cells transfected with scramble siRNA (Si Scramble) were able to completely fill the scratch wound by day 3 whereas ITGB4 knockdown cells (Si ITGB4) were not. **F)** H2009 and H1993 cells treated with 10 μM cisplatin over the course of 72 h. Data are represented as mean +/- SD.

Figure S5. ITGB4 knockdown induces cell death in NSCLC. Related to Figure 2.
A) Proliferation and apoptosis assays were executed with stable cell lines expressing nuclear RFP and the IncuCyte Caspase-3/7 Green Reagent (Essen BioScience), which emits green fluorescence when cleaved by activated caspase-3/7. Apoptosis is induced with knockdown of ITGB4 (Si ITGB4) by day 4 and enhanced with added cisplatin. **B)** In H1993 cells with ITGB4 knockdown (red), apoptosis increased significantly compared to control cells (black). **C)** ITGB4 knockdown and double knockdown of PXN and ITGB4 induced apoptosis in H1993 and rendered cells more prone to toxic effects of cisplatin. (*p=0.03, **p=0.002, ****p<0.0001 Two-way ANOVA) **D)** H2009 cells did not show significant increase in apoptosis with ITGB4 knockdown. **E)** Double knockdown of PXN and ITGB4 in H2009 cells induced strong apoptosis and in combination with cisplatin, caspase activity increased at an earlier time point of 24 h. (**p=0.02, ***p=0.0002, ****p<0.0001 Two-way ANOVA) **F)** Nuclear RFP-expressing cell line H1650 was transfected with ITGB4 siRNA (Si ITGB4) and monitored in real-time with the IncuCyte. Over the course of 10 h, ITGB4 knockdown induced cells with an intact membrane were observed to undergo anoikis-like bursting. **G)** ITGB4 knockdown (red) in H1650 cells attenuated cell proliferation compared to control (black). Data are represented as mean +/- SD.

Figure S6. ITGB4 knockdown enhances cisplatin sensitivity and double knockdown with PXN impedes spheroid viability. Related to Figure 3.
A) Effect of ITGB4 knockdown (3 different siITGB4 constructs) and cisplatin 2.5 μM on cell proliferation in H358 cells. **B)** Effect of ITGB4 knockdown (3 different siITGB4 constructs) and cisplatin 2.5 μM on cell proliferation in A549 cells. **C)** Expression of C-MET at the mRNA and protein level upon ITGB4 knockdown (red) compared to control (black). Data are represented as mean +/- SD.

Figure S7. PXN and ITGB4 knockdown induces caspase activity in spheroid culture. Related to Figure 3G-J.

A) H2009 cells expressing nuclear RFP were seeded in an ultra-low attachment 96-well plate to facilitate spheroid formation. After 4 h, double knockdown of PXN and ITGB4 impeded cells from forming a compact spheroid as observed in control and single knockdown conditions. **B)** and **C)** Spheroids with ITGB4 single knockdown and PXN/ITGB4 double knockdown were sensitized to cisplatin (10 μM) treatment indicated by a decrease in red fluorescence area and mean intensity. (****p<0.0001 Two-way ANOVA) **D)** In H2009 cells, single knockdown of ITGB4 (Si ITGB4) significantly induced apoptosis and double knockdown of PXN and ITGB4 (Si ITGB4+Si PXN) had an enhanced effect. (*p=0.014, ***p=0.0002) **E)** Double knockdown spheroids treated with cisplatin had the greatest cytotoxic effect indicated by the green fluorescence in the confocal images acquired by a Zeiss LSM 880 microscope. (**p<0.002, ***p<0.0009 Two-way ANOVA). Data are represented as mean +/- SD.

Figure S8. Control experiments for proximity ligation assay (PLA). Related to Figure 4F and G.
Each antibody (FAK, ITGB4, and PXN) used in the PLA experiment was tested separately as a negative control.

Figure S9. Supporting data for Figures 6-8. Related to Figures 6-8.
A) The selected constructs were tested for induction of caspase-3/7 activity by tracking green fluorescence using live cell imaging and analysis for 72 h. (****p<0.0001) **B)** H2009 and H1993 cells treated with ML323, a USP1 inhibitor, did not undergo significant changes in proliferation compared to untreated cells (black). **C)** Spare respiratory capacity, which is the ratio of maximal respiration vs. basal respiration, did not show any significant change between control and knockdown cells. **D)** RACIPE ensemble results (n=100,000) show ITGB4 and miR-1-3p exhibit bimodality: two distinct subpopulations of cells, as shown via z-score distributions of ITGB4 and miR-1-3p. **E)** FACS analysis using an anti-ITGB4 antibody showed enrichment of high ITGB4 population upon cisplatin treatment in H2009 cells. Data are represented as mean +/- SD. (****p<0.0001)

Figure S10. Knocking down ITGB4 with shRNA. Related to Figure 2.
A) Effect of knocking down ITGB4 with shRNA on cell proliferation over the course of 3 days. **B)** Images of H2009 cells stably transfected with plasmid pGFP-V-RS only or expressing ITGB4 shRNA at 20X magnification.

Table S1.

Original Member	Entrez Gene Id	Gene Symbol	Gene Description
AF010316	9536	PTGES	Prostaglandin E Synthase
AF019770	9518	GDF15	Growth Differentiation Factor 15
J04164	8519	IFITM1	Interferon Induced Transmembrane Protein 1
M29366	2065	ERBB3	V-erb-b2 Erythroblastic Leukemia Viral Oncogensis
M29870	5879	RAC1	Ras-related C3 Botulinum Toxin Substrate 1
M33882	4599	MX1	Myxovirus (Influenza Virus) Resistance 1
S80437	2194	FASN	Fatty Acid Synthase
U09579	1026	CDKN1A	Cyclin-dependent Kinase Inhibitor 1A
U14588	5829	PXN	Paxillin
X53587	3691	ITGB4	Integrin, Beta 4
X74295	3679	ITGA7	Integrin, Alpha 7

Table S2.

	Estimate	Standard Error	Relative Risk	P-Value
gender[1]	- 0.04918	0.154775	0.952008	0.750665
stage[S2]	0.738091	0.194204	2.09194	0.000144
stage[S3]	1.17346	0.192492	3.23316	1.09E-09
stage[S4]	1.31524	0.284479	3.72563	3.78E-06
age	2.36E-05	2.14E-05	1.00002	0.271914
ENSG00000089159* ENSG00000132470	0.000156	3.03E-05	1.00016	2.47E-07

Table S3.

Category	Term	Fold Enrichment	Count	PValue
GOTERM_BP_DIRECT	GO:0006355~regulation of transcription, DNA-templated	2.232978723	17	0.0029
GOTERM_BP_DIRECT	GO:0003158~endothelium development	65.85098039	2	0.0296
GOTERM_BP_DIRECT	GO:0000086~G2/M transition of mitotic cell cycle	5.767969085	4	0.0314
GOTERM_BP_DIRECT	GO:0006351~transcription, DNA-templated	1.717851662	17	0.0316
GOTERM_BP_DIRECT	GO:0015677~copper ion import	56.44369748	2	0.0345
GOTERM_BP_DIRECT	GO:0002544~chronic inflammatory response	43.90065359	2	0.0441
GOTERM_BP_DIRECT	GO:0007156~homophilic cell adhesion via plasma membrane adhesion molecules	5.001340283	4	0.0448
KEGG_PATHWAY	hsa04350:TGF-beta signaling pathway	8.471674877	3	0.0454
KEGG_PATHWAY	hsa00450:Selenocompound metabolism	27.90669371	2	0.0671
GOTERM_BP_DIRECT	GO:0001701~in utero embryonic development	4.225731362	4	0.0673
GOTERM_BP_DIRECT	GO:0008284~positive regulation of cell proliferation	2.543600101	6	0.0841
GOTERM_BP_DIRECT	GO:0010971~positive regulation of G2/M transition of mitotic cell cycle	21.9503268	2	0.0864

Table S4.

Category	Term	Fold Enrichment	Count	PValue
GOTERM_BP_DIRECT	GO:0006334~nucleosome assembly	5.759560967	8	4.79E-04
GOTERM_BP_DIRECT	GO:0007265~Ras protein signal transduction	6.119533528	5	0.00891
KEGG_PATHWAY	hsa04810:Regulation of actin cytoskeleton	3.04717608	8	0.01475
GOTERM_BP_DIRECT	GO:0001525~angiogenesis	3.073487691	8	0.01553
KEGG_PATHWAY	hsa05034:Alcoholism	3.163381947	7	0.02182
GOTERM_BP_DIRECT	GO:0017085~response to insecticide	85.67346939	2	0.02309
KEGG_PATHWAY	hsa05322:Systemic lupus erythematosus	3.5815689	6	0.02467
GOTERM_BP_DIRECT	GO:0032091~negative regulation of protein binding	6.01217329	4	0.02854
KEGG_PATHWAY	hsa04070:Phosphatidylinositol signaling system	4.081039393	5	0.03263
GOTERM_BP_DIRECT	GO:0060978~angiogenesis involved in coronary vascular morphogenesis	57.11564626	2	0.03444
GOTERM_BP_DIRECT	GO:0006203~dGTP catabolic process	57.11564626	2	0.03444
GOTERM_BP_DIRECT	GO:0045815~positive regulation of gene expression, epigenetic	5.527320606	4	0.03538
GOTERM_BP_DIRECT	GO:0009611~response to wounding	5.439585358	4	0.03684
GOTERM_BP_DIRECT	GO:0043928~exonucleolytic nuclear-transcribed mRNA catabolic process involved in deadenylation-dependent decay	8.862772695	3	0.04437
GOTERM_BP_DIRECT	GO:0035404~histone-serine phosphorylation	42.83673469	2	0.04565
GOTERM_BP_DIRECT	GO:0007052~mitotic spindle organization	8.567346939	3	0.04718
GOTERM_BP_DIRECT	GO:0030855~epithelial cell differentiation	4.895626822	4	0.04791
GOTERM_BP_DIRECT	GO:0006335~DNA replication-dependent nucleosome assembly	8.031887755	3	0.053
GOTERM_BP_DIRECT	GO:0061551~trigeminal ganglion development	34.26938776	2	0.05674
KEGG_PATHWAY	hsa04152:AMPK signaling pathway	3.251559841	5	0.06526
GOTERM_BP_DIRECT	GO:0042060~wound healing	4.283673469	4	0.06621
GOTERM_BP_DIRECT	GO:0032958~inositol phosphate biosynthetic process	28.55782313	2	0.06769
GOTERM_BP_DIRECT	GO:0071455~cellular response to hyperoxia	24.47813411	2	0.07852
GOTERM_BP_DIRECT	GO:0051290~protein heterotetramerization	6.119533528	3	0.08541
GOTERM_BP_DIRECT	GO:0007160~cell-matrix adhesion	3.807709751	4	0.08722
GOTERM_BP_DIRECT	GO:0051597~response to methylmercury	21.41836735	2	0.08923
GOTERM_BP_DIRECT	GO:0030514~negative regulation of BMP signaling pathway	5.711564626	3	0.09605
GOTERM_BP_DIRECT	GO:0060627~regulation of vesicle-mediated transport	19.03854875	2	0.09981
GOTERM_BP_DIRECT	GO:0030903~notochord development	19.03854875	2	0.09981

Table S5.

	Activation Score	Predicted Activation	P-value
ITGB4 Knockdown			
miR-223	2.236	Activated	0.0985
miR-210	2.449	Activated	0.00772
miR-124-3p	2.077	Activated	0.00352
miR-1-3p	3.128	Activated	0.0000133
PXN KD			
miR-199a-5p	-2.43	Inhibited	0.000731
PXN/ITGB4 Knockdown			
miR-291a-3p	2.562	Activated	1.25E-08
miR-124-3p	2.292	Activated	0.0000371
miR-30c-5P	2.345	Activated	0.0081
miR-1-3p	2.543	Activated	0.00296
miR-199a-5p	-2.135	Inhibited	0.0015

Table S6.

siRNA Sequence

Target Gene	**Locus ID**	**RefSeq**	**Construct**	**Sequence (5'-3')**
PXN	5829	NM_001080855.2, NM_001243756.1, NM_002859.3, NM_025157.4	-	GCUUCGCUGUCGGAUUUCATT
ITGB4	3691	NM_000213, NM_001005619, NM_001005731, NM_001321123	A	CAGUUCUGCGAGUAUGACAACUUCC
			B	CGAGAAGCUUCACACCUAUUUCCCT
			C*	GUCAGUUCUGCGAGUAUGACAACTT
USP1	7398	NM_001017415, NM_001017416, NM_003368	A	AGCUACAAGUGAUACAUUAGAGAGT
			B*	GGAGCACAAAGCCAACUAACGARCAG
			C	GGCAAGUUAUGAAUUGAUAUGCAGT
VDAC1	7416	NM_003374, NR_036624, NR_036625	A*	ACAACACUCAGAAUCUAAAUUGGAC
			B	GGAAUUUCAAGCAUAAAUGAAUACT
			C	GCACCAGAGUAUGAAAUAGCUUCCA
ITGA7	3679	NM_001144996, NM_001144997, NM_002206	A	AGUGAAGUCCUCCAUAAAGAACUTG
			B	GUAUGAGGUCACGGUUUCCAACCAA
			C	CUUAGUUUGCUGCCAUCAGUCUAGT
KIF14	9928	NM_001305792, NM_014875	A	GCACUGACAAGAAAUGUUAUAAAGA
			B	CACGAUCACAGAAUAACAAGUCGAA
			C	GGCAUAACUAGUUGAAAUUGGCCAT
G3BP1	10146	NM_005754, NM_198395	A	GUGCGAGAACAACGAAUAAAUAUTC
			B	CCCGUAAGAAGGAAUGUUACUUUAA
			C	ACCACCUCAUGUUGUUAAAGUACCA

* Denotes optimal siRNA construct used for downstream experiments

Fig. S1

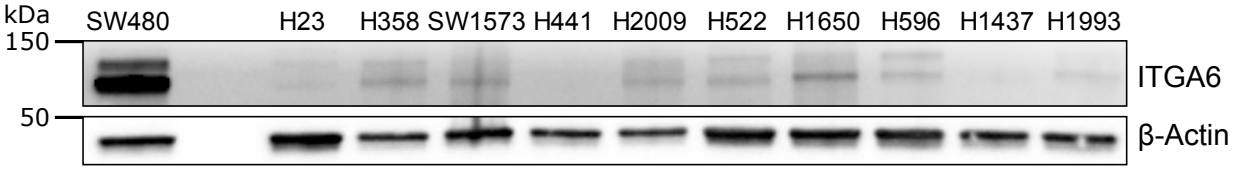
kDa
150
50
SW480
H23
H358
SW1573
H441
H2009
H522
H1650
H596
H1437
H1993
ITGA6
β-Actin

Fig. S2

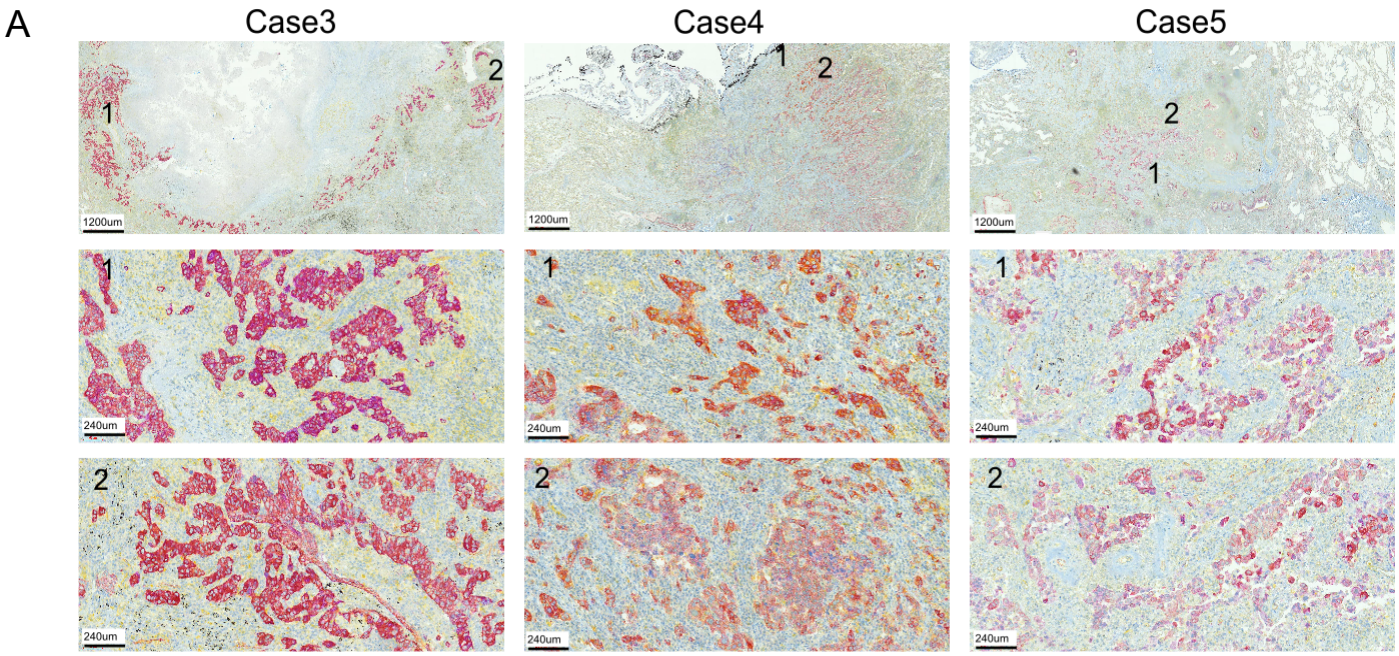
A
Case3
Case4
Case5
1
2
1200um
240um

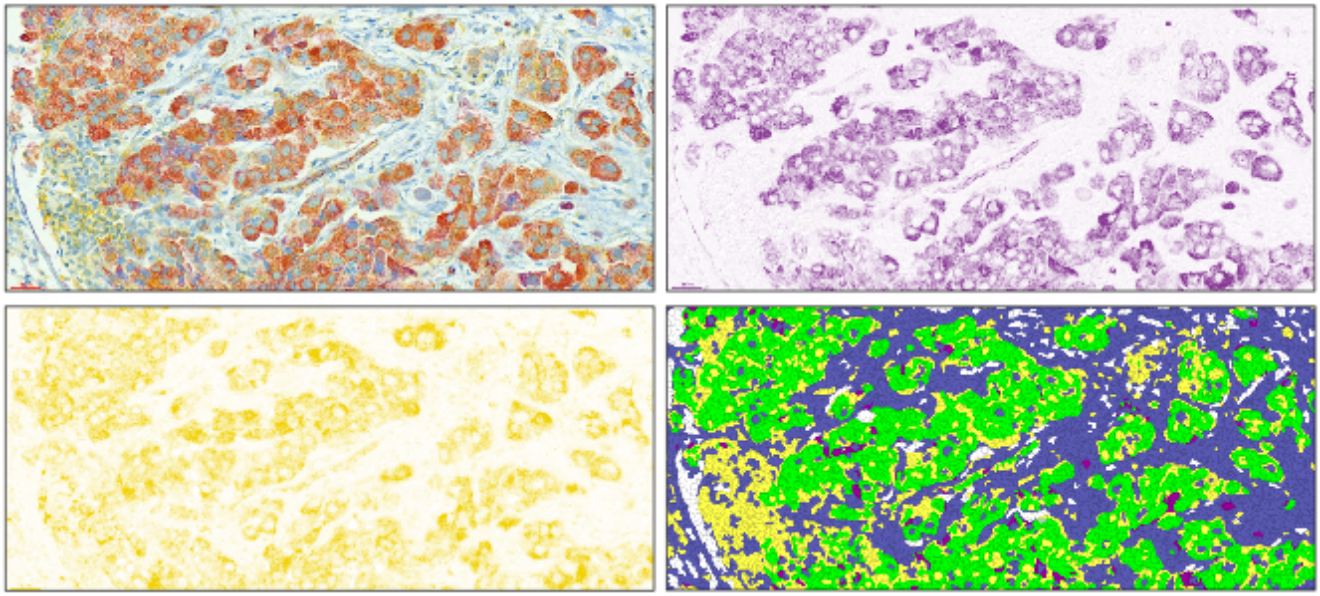
B

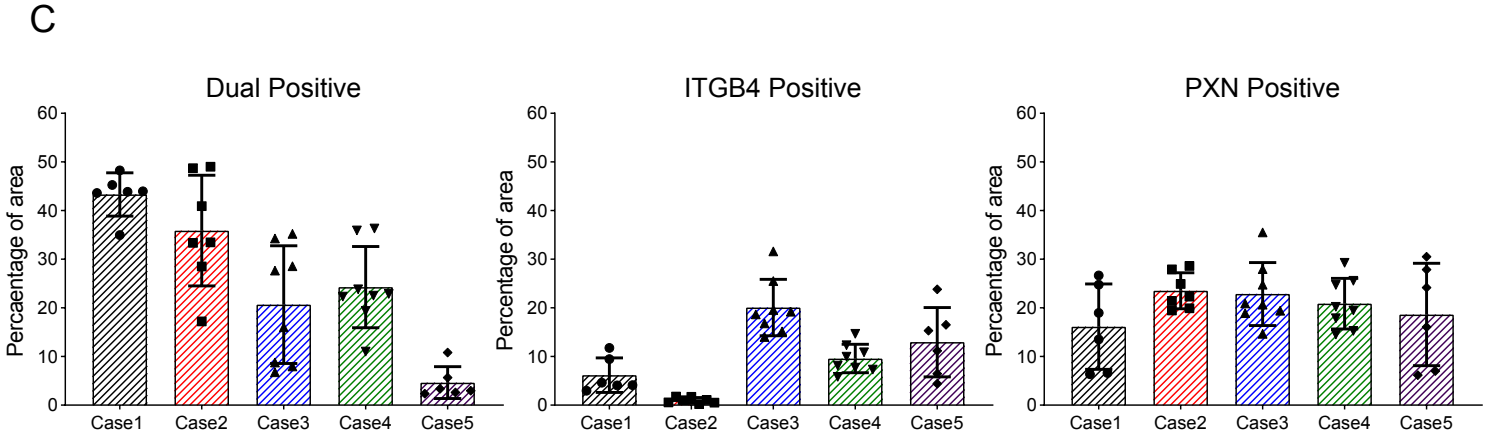
C
Dual Positive
ITGB4 Positive
PXN Positive
Percaentage of area
Percentage of area
0
10
20
30
40
50
60
Case1
Case2
Case3
Case4
Case5

Fig. S3

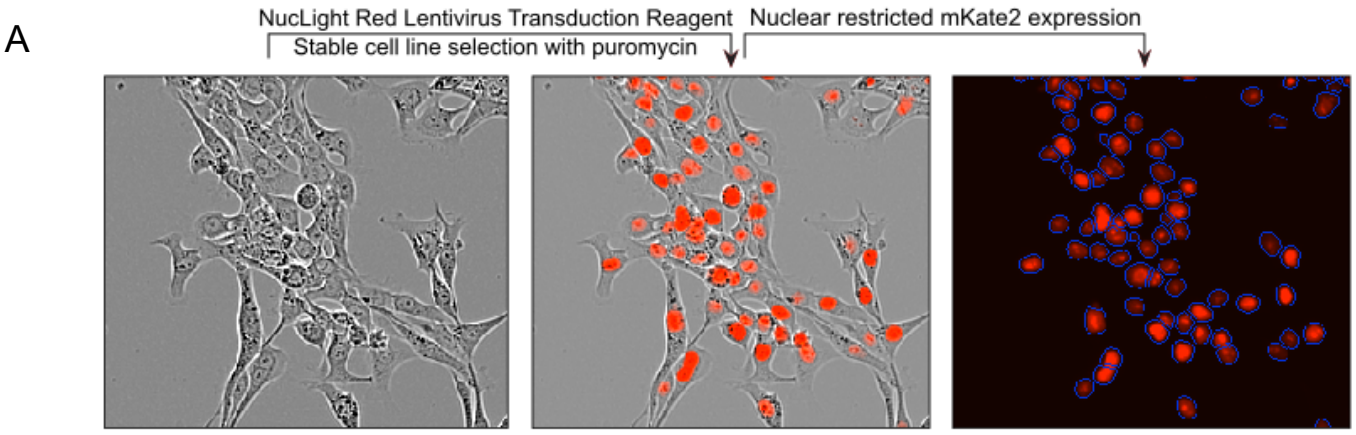
A
NucLight Red Lentivirus Transduction Reagent
Stable cell line selection with puromycin
Nuclear restricted mKate2 expression

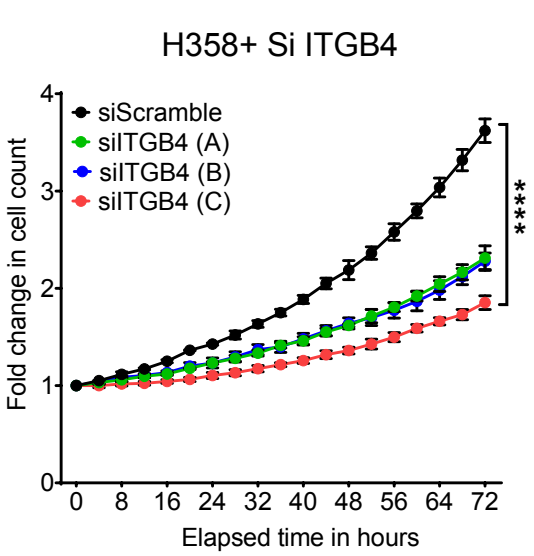
B
H358+ Si ITGB4
siScramble
siITGB4 (A)
siITGB4 (B)
siITGB4 (C)
Fold change in cell count
Elapsed time in hours
****

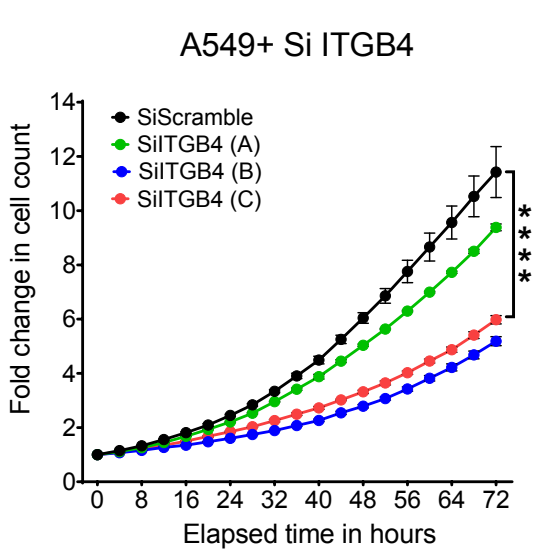
C
A549+ Si ITGB4
SiScramble
SiITGB4 (A)
SiITGB4 (B)
SiITGB4 (C)
Fold change in cell count
Elapsed time in hours
****

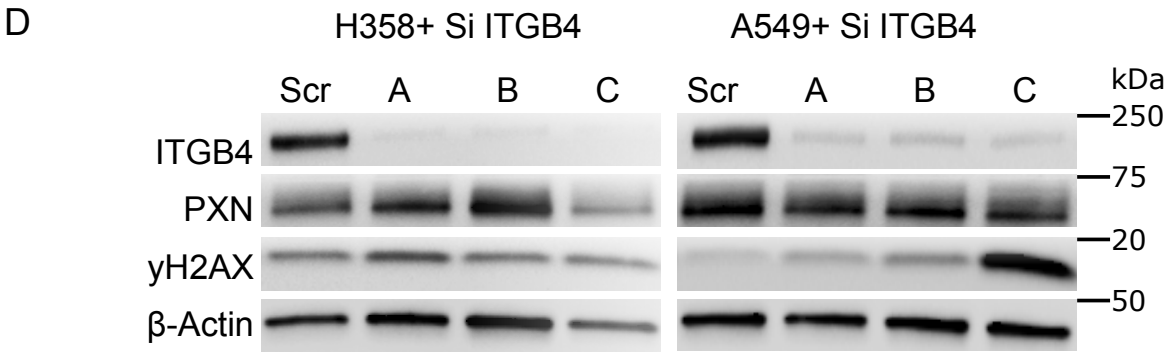
D
H358+ Si ITGB4
A549+ Si ITGB4
Scr
A
B
C
kDa
ITGB4
PXN
yH2AX
β-Actin
250
75
20
50

Fig. S4

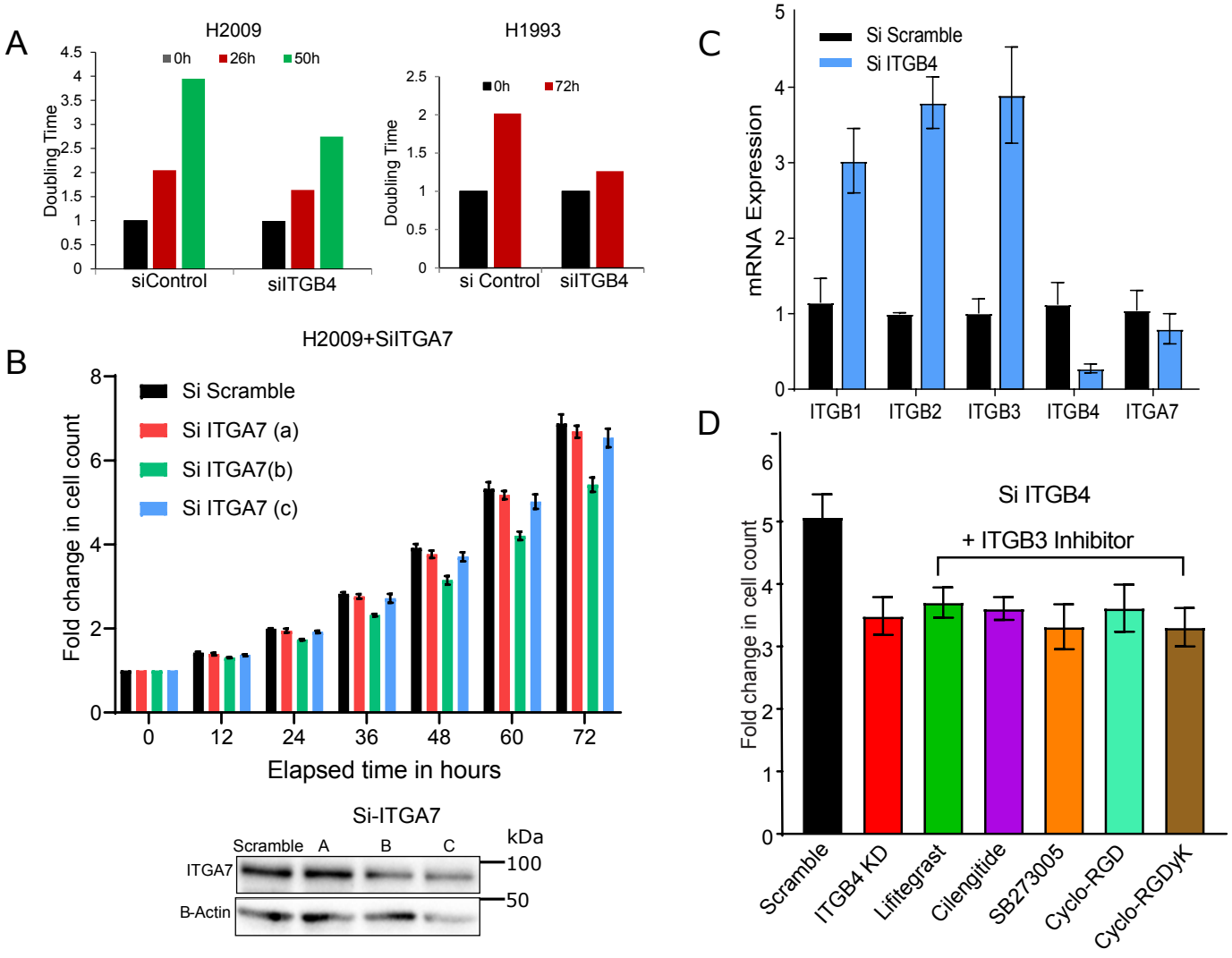
A
H2009
0h
26h
50h
Doubling Time
siControl
siITGB4
H1993
0h
72h
Doubling Time
si Control
siITGB4
B
H2009+SiITGA7
Si Scramble
Si ITGA7 (a)
Si ITGA7(b)
Si ITGA7 (c)
Fold change in cell count
Elapsed time in hours
Si-ITGA7
Scramble
A
B
C
kDa
ITGA7
B-Actin
100
50
C
Si Scramble
Si ITGB4
mRNA Expression
ITGB1
ITGB2
ITGB3
ITGB4
ITGA7
D
Si ITGB4
+ ITGB3 Inhibitor
Fold change in cell count
Scramble
ITGB4 KD
Lifitegrast
Cilengitide
SB273005
Cyclo-RGD
Cyclo-RGDyK

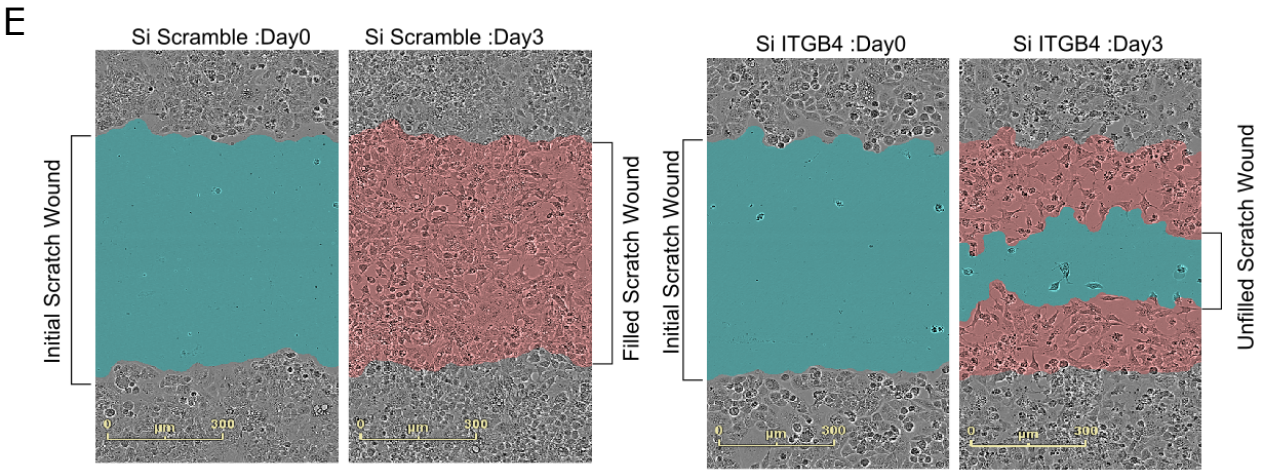
E
Si Scramble :Day0
Si Scramble :Day3
Initial Scratch Wound
Filled Scratch Wound
Si ITGB4 :Day0
Si ITGB4 :Day3
Initial Scratch Wound
Unfilled Scratch Wound

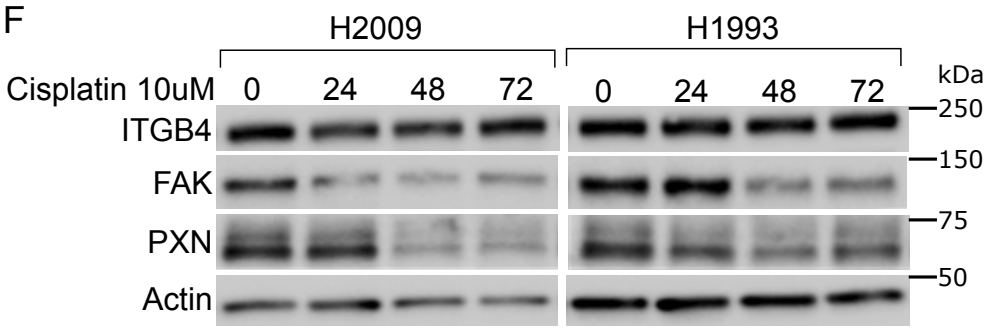
F
H2009
H1993
Cisplatin 10uM
0
24
48
72
0
24
48
72
kDa
ITGB4
FAK
PXN
Actin
250
150
75
50

Fig. S5

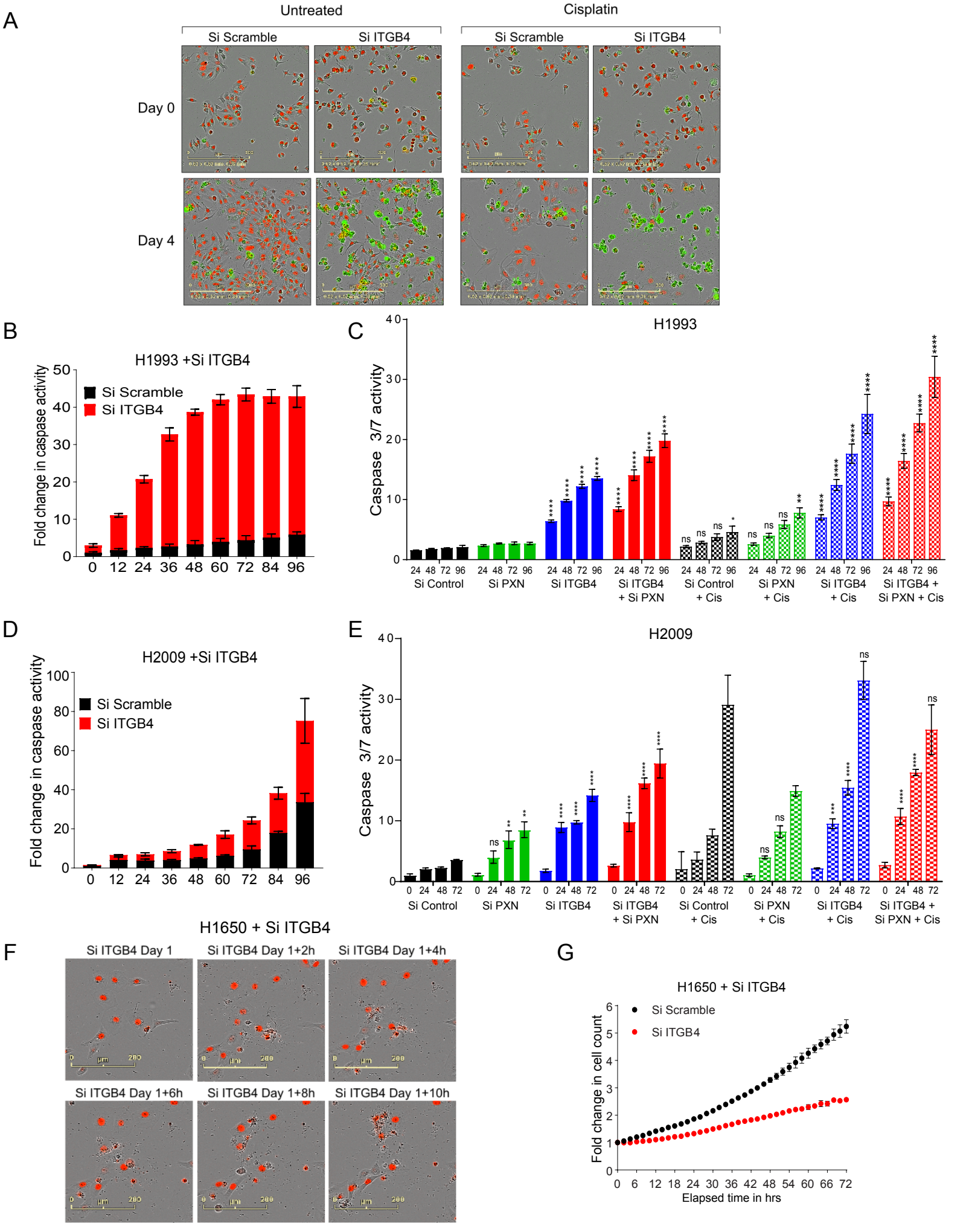
A
Untreated
Cisplatin
Si Scramble
Si ITGB4
Si Scramble
Si ITGB4
Day 0
Day 4
B
H1993 +Si ITGB4
Si Scramble
Si ITGB4
Fold change in caspase activity
0 12 24 36 48 60 72 84 96
C
H1993
Caspase 3/7 activity
24 48 72 96
Si Control
Si PXN
Si ITGB4
Si ITGB4 + Si PXN
Si Control + Cis
Si PXN + Cis
Si ITGB4 + Cis
Si ITGB4 + Si PXN + Cis
D
H2009 +Si ITGB4
Si Scramble
Si ITGB4
Fold change in caspase activity
0 12 24 36 48 60 72 84 96
E
H2009
Caspase 3/7 activity
0 24 48 72
Si Control
Si PXN
Si ITGB4
Si ITGB4 + Si PXN
Si Control + Cis
Si PXN + Cis
Si ITGB4 + Cis
Si ITGB4 + Si PXN + Cis
F
H1650 + Si ITGB4
Si ITGB4 Day 1
Si ITGB4 Day 1+2h
Si ITGB4 Day 1+4h
Si ITGB4 Day 1+6h
Si ITGB4 Day 1+8h
Si ITGB4 Day 1+10h
G
H1650 + Si ITGB4
Si Scramble
Si ITGB4
Fold change in cell count
0 6 12 18 24 30 36 42 48 54 60 66 72
Elapsed time in hrs

Fig. S6

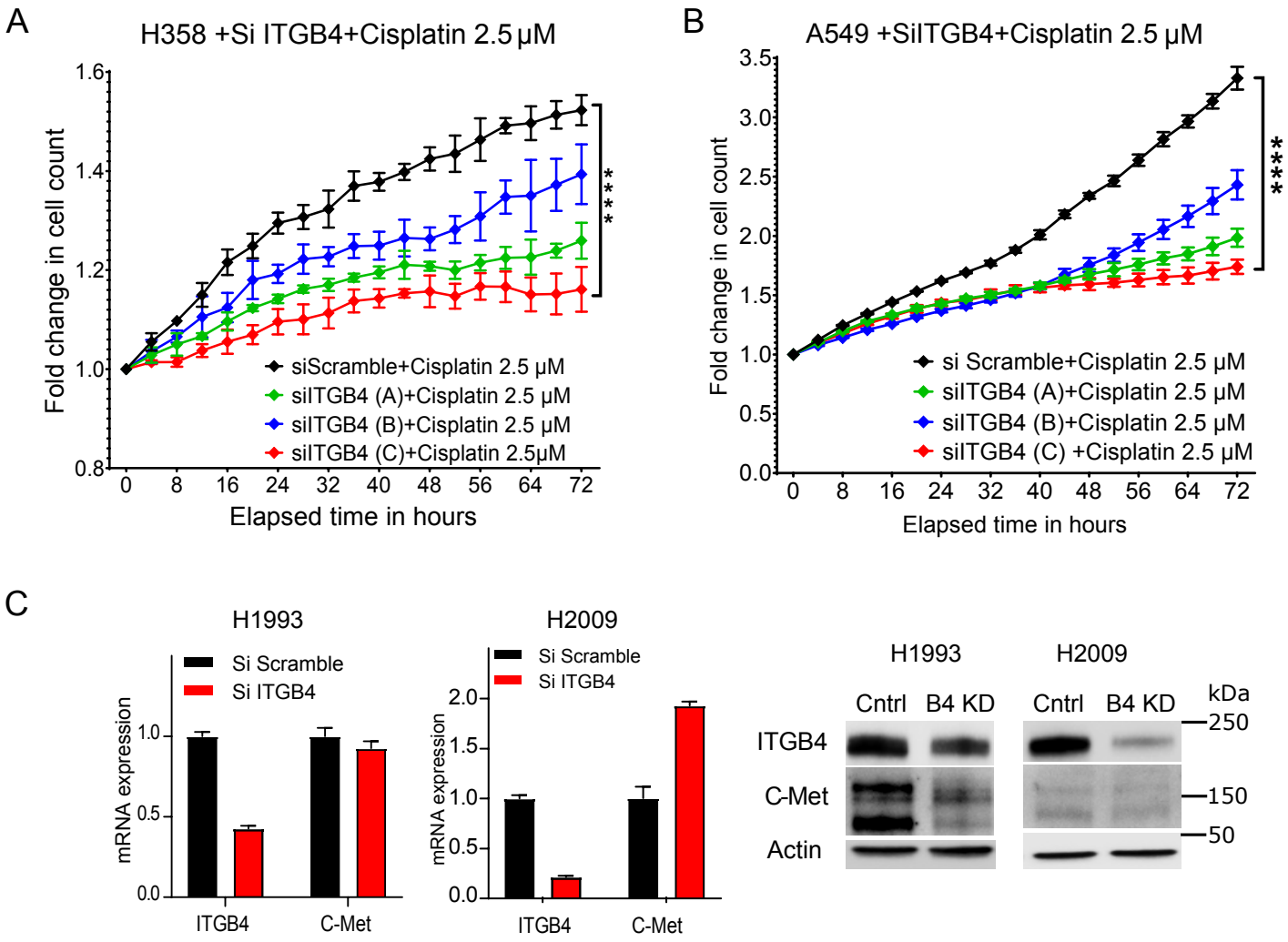
A
H358 +Si ITGB4+Cisplatin 2.5 µM
Fold change in cell count
Elapsed time in hours
siScramble+Cisplatin 2.5 µM
siITGB4 (A)+Cisplatin 2.5 µM
siITGB4 (B)+Cisplatin 2.5 µM
siITGB4 (C)+Cisplatin 2.5µM
****
B
A549 +SiITGB4+Cisplatin 2.5 µM
Fold change in cell count
Elapsed time in hours
si Scramble+Cisplatin 2.5 µM
siITGB4 (A)+Cisplatin 2.5 µM
siITGB4 (B)+Cisplatin 2.5 µM
siITGB4 (C) +Cisplatin 2.5 µM
****
C
H1993
H2009
Si Scramble
Si ITGB4
mRNA expression
ITGB4
C-Met
H1993
H2009
Cntrl
B4 KD
Cntrl
B4 KD
kDa
ITGB4
C-Met
Actin
250
150
50

Fig. S7

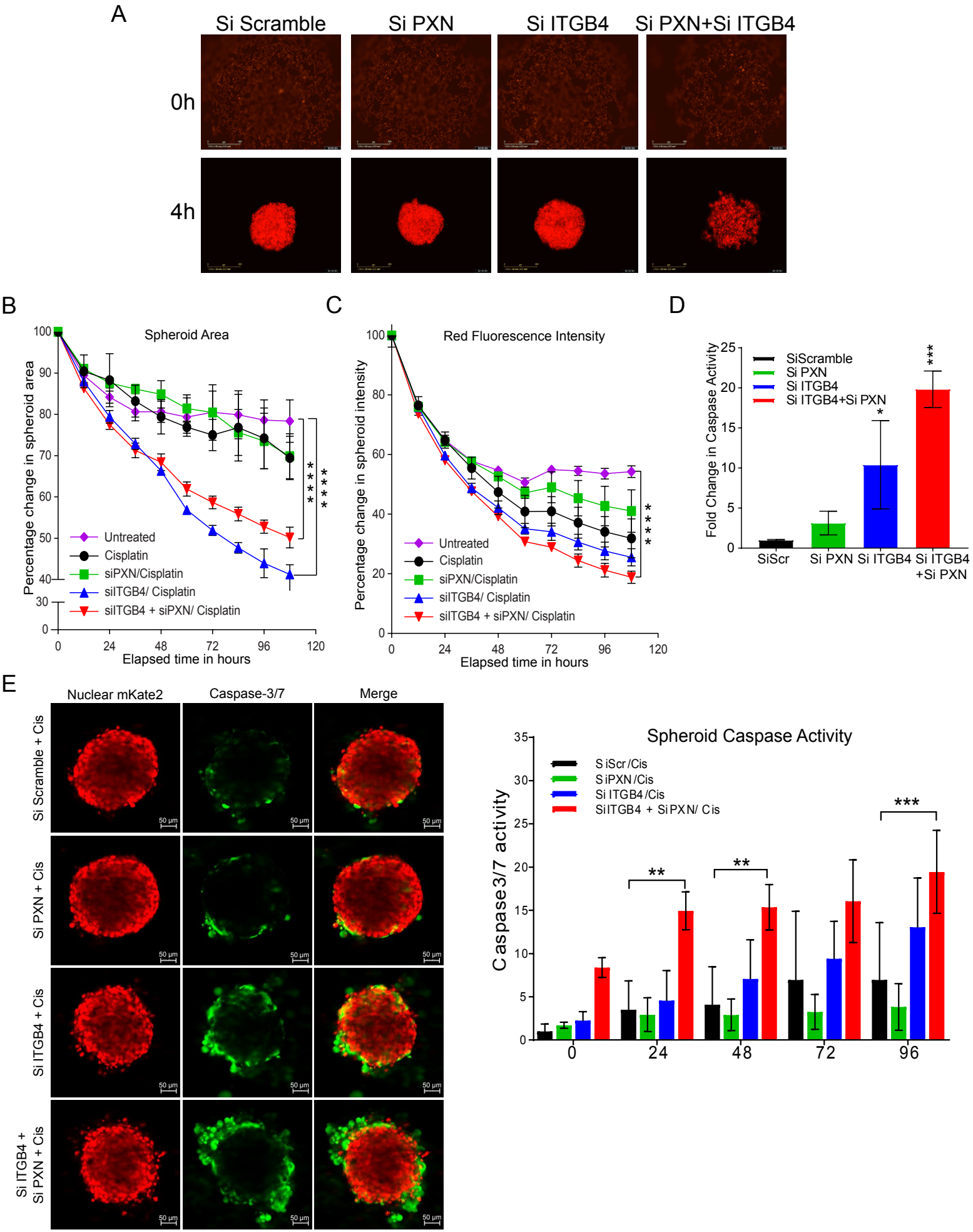
A
Si Scramble
Si PXN
Si ITGB4
Si PXN+Si ITGB4
0h
4h
B
Spheroid Area
Percentage change in spheroid area
Elapsed time in hours
Untreated
Cisplatin
siPXN/Cisplatin
siITGB4/ Cisplatin
siITGB4 + siPXN/ Cisplatin
****
C
Red Fluorescence Intensity
Percentage change in spheroid intensity
Elapsed time in hours
Untreated
Cisplatin
siPXN/Cisplatin
siITGB4/ Cisplatin
siITGB4 + siPXN/ Cisplatin
****
D
Fold Change in Caspase Activity
SiScramble
Si PXN
Si ITGB4
Si ITGB4+Si PXN
*
***
SiScr
Si PXN
Si ITGB4
Si ITGB4 +Si PXN
E
Nuclear mKate2
Caspase-3/7
Merge
Si Scramble + Cis
Si PXN + Cis
Si ITGB4 + Cis
Si ITGB4 + Si PXN + Cis
50 µm
Spheroid Caspase Activity
Caspase3/7 activity
SiScr/Cis
SiPXN/Cis
Si ITGB4/Cis
SiITGB4 + SiPXN/ Cis
**
**
***

Fig. S8

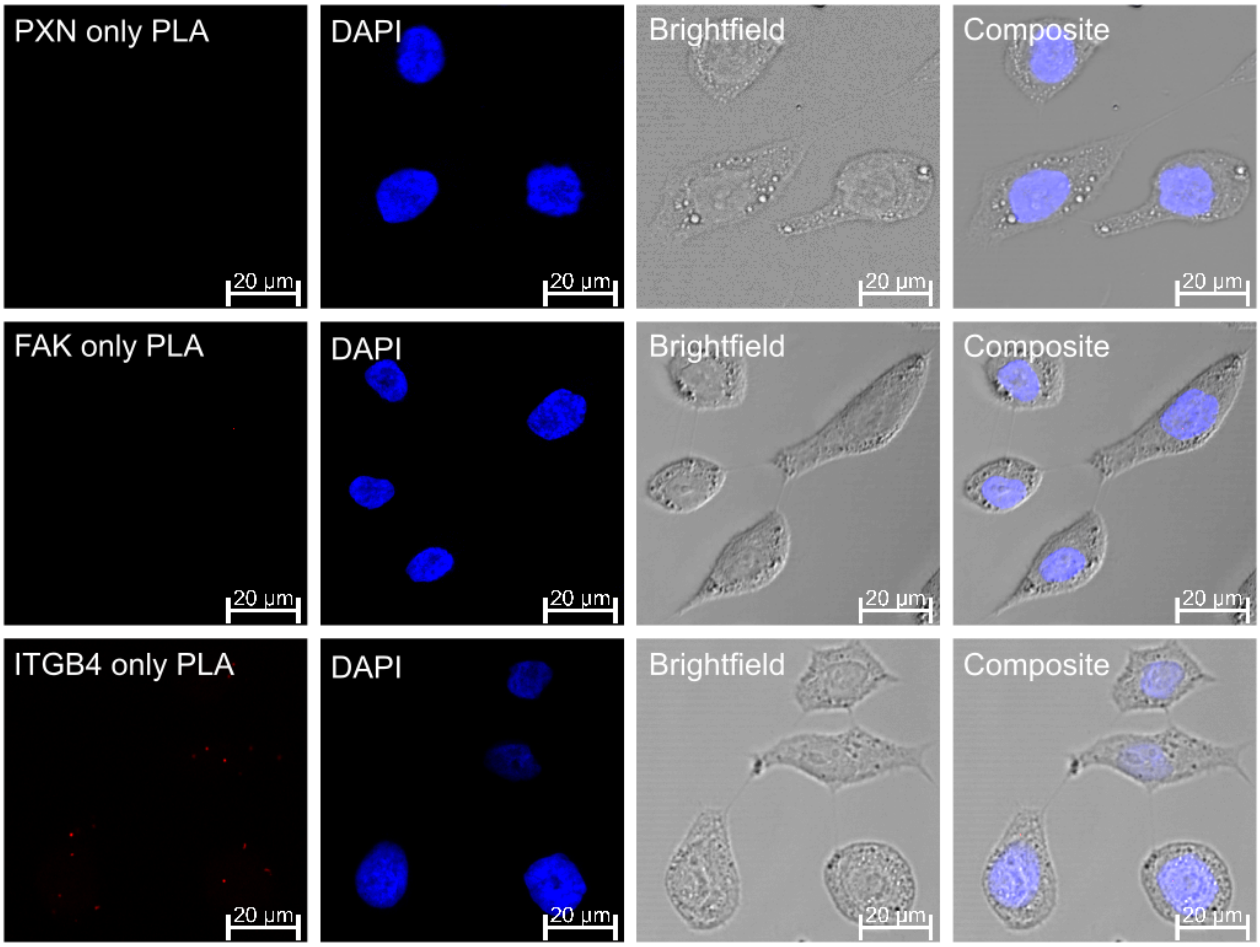
PXN only PLA
DAPI
Brightfield
Composite
FAK only PLA
DAPI
Brightfield
Composite
ITGB4 only PLA
DAPI
Brightfield
Composite
20 µm

Fig. S9

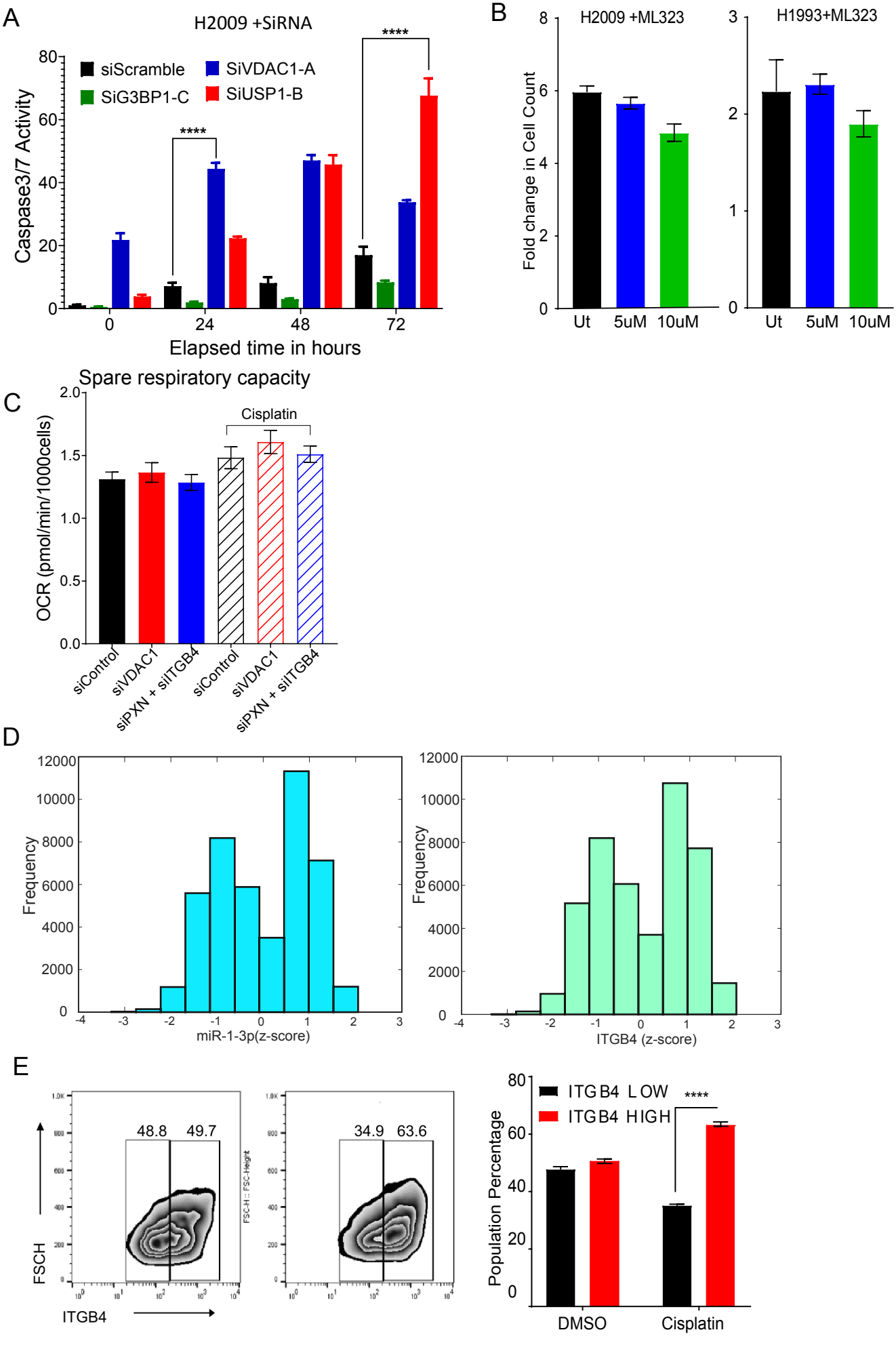
A
H2009 +SiRNA
siScramble
SiVDAC1-A
SiG3BP1-C
SiUSP1-B
Caspase3/7 Activity
Elapsed time in hours
****
****
B
H2009 +ML323
H1993+ML323
Fold change in Cell Count
Ut
5uM
10uM
C
Spare respiratory capacity
Cisplatin
OCR (pmol/min/1000cells)
siControl
siVDAC1
siPXN + siITGB4
D
Frequency
miR-1-3p(z-score)
ITGB4 (z-score)
E
48.8
49.7
34.9
63.6
FSCH
ITGB4
ITGB4 LOW
ITGB4 HIGH
Population Percentage
DMSO
Cisplatin

Fig. S10

A

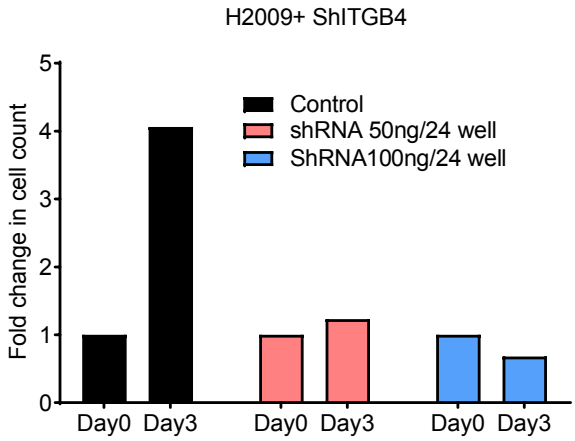
H2009+ ShITGB4
Fold change in cell count
0
1
2
3
4
5
Control
shRNA 50ng/24 well
ShRNA100ng/24 well
Day0
Day3
Day0
Day3
Day0
Day3

B

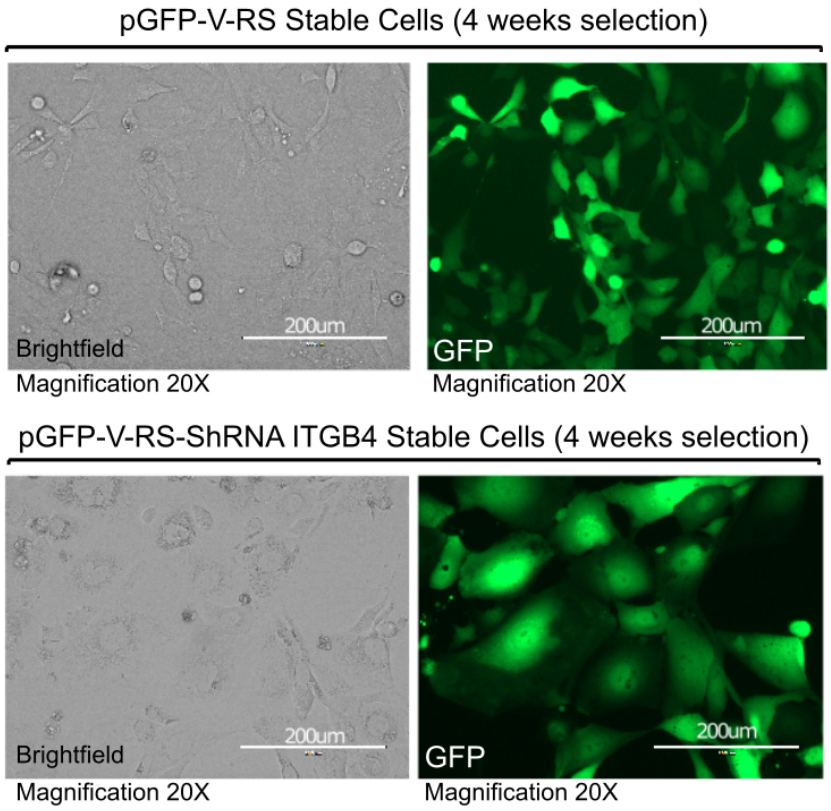
pGFP-V-RS Stable Cells (4 weeks selection)
Brightfield
200um
Magnification 20X
GFP
200um
Magnification 20X
pGFP-V-RS-ShRNA ITGB4 Stable Cells (4 weeks selection)
Brightfield
200um
Magnification 20X
GFP
200um
Magnification 20X

Transparent Methods

Cell lines and reagents

Lung cancer cell lines (A549, H23, H358, SW1573, H441, H2009, H522, H1650, H596, H1437, and H1993) were obtained from American Type Culture Collection (ATCC) (Manassas, VA, USA). All cell lines were cultured in RPMI 1640 medium (Corning) supplemented with fetal bovine serum (FBS) (10%), L-glutamine (2 mM), penicillin/streptomycin (50 U/ml), sodium pyruvate (1 mM), and sodium bicarbonate (0.075%) at 37°C, 5% CO_2. Cisplatin was provided by City of Hope National Medical Center clinics.

Antibodies

Antibodies against ITGB4 (cat #: 4707), FAK (cat #: 3285), phospho-FAK (Y397) (cat #: 8556), γH2AX (cat #: 2557), p27 (cat #: 3686), phospho-Rb (S807/811) (cat #: 8516), USP1 (cat #: 8033), and ITGA6 (cat #: 3750) were purchased from Cell Signaling Technology (Danvers, MA, USA). Antibodies against ITGA7 (cat #: sc-515716), ITGA6 (cat #: sc-53356), PXN (cat #: sc-5574), MET (cat #: sc-10), G3BP1 (cat #: sc-365338), and VDAC1 (cat #: sc-390996) , and agarose-conjugated antibodies (ITGB4, FAK, PXN, IgG) were purchased from Santa Cruz Biotechnology (Dallas, TX, USA). Cyclin D1 antibody was purchased from Invitrogen (cat #: MA5-14512) (Waltham, MA, USA). Phospho-PXN (Y31) (cat #: ab4832) antibody was purchased from Abcam (Cambridge, UK). β-actin antibody was purchased from Sigma-Aldrich (cat #: A5441) (St. Louis, MO, USA).

Western blotting

Cell lysates were prepared with 1X RIPA buffer (MilliporeSigma) and denatured in 1X reducing sample buffer at 95°C for 5 min. Protein samples (15 μg) were run on 4-15% TGX gels (Bio-Rad, Hercules, CA, USA) and transferred onto nitrocellulose membranes (Bio-Rad). Blots were blocked with 5% non-fat milk in TBS-T for 1 hour at room temperature and probed with primary antibody diluted in 2.5% BSA in TBS-T overnight at 4°C. After three washes with TBS-T, blots were incubated with HRP-conjugated secondary antibodies for 2 hours at room temperature. After three more washes, bands of interest were visualized via chemiluminescence using WesternBright ECL HRP substrate (Advansta, Menlo Park, CA, USA) and imaged with the ChemiDoc MP imager (Bio-Rad).

Quantitative real-time PCR and RNAseq

Quantitative real-time PCR (qPCR) reactions were performed using TaqMan Universal PCR Master Mix (Thermo Fisher Scientific, Waltham, MA) and analyzed by the Quant Studio7 Real-time PCR system (Life Technologies, Grand Island, NY). Total RNA isolation and on-column DNase digestion from cells were performed basing on the manufacturer's protocol RNeasy Plus Mini Kit (Qiagen Cat #: 74134). 1 ug of RNA was used to synthesize the cDNA according to the one step cDNA synthesis kit from QuantaBio (Cat#: 101414-106). TaqMan probes for HS99999905 –GAPDH, HS00236216-ITGB4, HS01104424-PXN, HS00174397-ITGB1, HS00164957-ITGB2,

HS01001469-ITGB3, HS01565584-MET, HS04978484-VDAC1, HS00428478-G3BP1 and HS00163427-USP1 were purchased from ThermoFisher (Waltham, MA). The mRNA expression was analyzed using multiplex PCR for the gene of interest and GAPDH as reference using two independent detection dyes FAM probes and VIC probes respectively. Relative mRNA expression was normalized to GAPDH signals and calculated using the delta delta Ct method.

RNA was extracted from both single and double knockdown H2009 cells 48 h post siRNA transfection, and total RNAseq was performed by the Integrative Genomics Core at City of Hope. RSeQC showed no substantial bias in the coverage of RNAseq reads. A total of 30 million reads were analyzed for each condition.

siRNA and shRNA Transfection

Knockdown of ITGB4 (Cat #: SR302473C), FAK (Cat #: SR303877C), USP1 (Cat #: SR305052B), and VDAC1 (Cat #: SR305067C) at the mRNA level was executed using siRNAs purchased from OriGene Technologies (Rockville, MD, USA). Knockdown of PXN was achieved by siRNA purchased from Life Technologies Corporation (Cat #: 4392421). JetPRIME transfection reagent (Polyplus Transfection, Illkirch, France) was used to transfect the siRNAs according to the manufacturer's protocol. Cells were seeded in 6-well plates (200,000 cells/well) and allowed to adhere overnight. Next day, 10 nM siRNA was transfected with 4 µl jetPRIME reagent in complete growth medium for each well. Cell growth medium was changed the next day and expression was detected 72 h post-transfection by immunoblot. Similarly, the plasmid pGFP-V-RS expressing shRNA against ITGB4 was used to transfect H2009 cells, and puromycin (ThermoFisher) was used to generate a stable cell line. The sequences of all the siRNAs used are described in **Table S6**.

Cell viability assay

Cell Counting Kit-8 (CCK-8) was purchased from Dojindo Molecular Technologies (Rockville, MD, USA). Cells were seeded on a 96-well plate and allowed to adhere in complete medium for 24 hours. Test compounds were added to 100 µl of medium at the indicated concentrations for 72 hours. Ten µl of the CCK-8 reagent were added to each well and absorbance at 450 nm was measured using a Tecan Spark 10M multimode microplate reader.

Immunohistochemistry (IHC)

Dual IHC stain for ITGB4 and PXN was performed on Ventana Discovery Ultra (Ventana Medical Systems, Roche Diagnostics, Indianapolis, USA) automated IHC stainer. Briefly, tissue samples were sectioned at a thickness of 5 µm and mounted on positively charged glass slides. The slides were loaded on the machine and deparaffinization, rehydration, endogenous peroxidase activity inhibition and antigen retrieval were performed. Then, the two antigens were sequentially detected, and heat inactivation was used to prevent antibody cross-reactivity between the same species. Following each primary antibody incubation, DISCOVERY anti-mouse HQ or DISCOVERY anti-Rabbit NP and DISCOVERY anti-HQ-HRP or anti-NP-AP were incubated. The stains were then visualized with DISCOVERY Purple and DISCOVERY Yellow Kit, respectively,

counterstained with hematoxylin (Ventana) and cover slipped. The slides were scanned using the Motic Easy Scanner and 40X images were analyzed using the QuPath software.

Scratch wound healing assay

Cells were seeded on a 96-well ImageLock (Essen BioScience, Ann Arbor, MI, USA) plate to reach 90% confluence by the next day. After cell adherence, 96 uniform wounds were created simultaneously using the WoundMaker (Essen BioScience) tool. Cells were washed once with serum-free medium and replenished with complete medium. To monitor wound healing, the plate was placed in the IncuCyte S3 Live Cell Imaging System (Essen BioScience) and images were acquired every hour. Data analysis was generated by the IncuCyte software using a set confluence mask to measure relative wound density over time.

Cell proliferation and apoptosis assay

Cell proliferation assays were performed using cell lines stably transfected with NucLight Red Lentivirus (Essen BioScience) to accurately visualize and count the nucleus of a single cell. Cells were seeded on a 96-well plate and allowed to adhere for 24 h. Test compounds were added at indicated concentrations. Caspase-3/7 Green Apoptosis Reagent (Essen BioScience) was also added as a green fluorescent indicator of caspase-3/7-mediated apoptotic activity. To monitor cell proliferation and apoptosis over time, the plate was placed in the IncuCyte S3 Live Cell Imaging System (Essen BioScience) and images were acquired every 2 hours. Data analysis was generated by the IncuCyte software using a red fluorescence mask to accurately count each cell nucleus and a green fluorescence mask to measure apoptosis over time.

3D spheroid assay

3D spheroid experiments were performed using cell lines stably transfected with NucLight Red Lentivirus (Essen BioScience) to visualize red fluorescence as an indicator of cell viability. Cells were seeded on a 96-well ultra-low attachment plate and allowed to form spheroids overnight. Drug treatment was added as indicated along with Cytotox Green Reagent (Essen BioScience), used as a green fluorescence indicator of cell death due to loss of cell membrane integrity. To monitor cell proliferation and apoptosis over time, the plate was placed in the IncuCyte S3 Live Cell Imaging System (Essen BioScience) and images were acquired every 2 hours. Data analysis was generated by the IncuCyte software using a red fluorescence mask to accurately measure intensity and area of red fluorescence, indicating spheroid viability and a green fluorescence mask, indicating cell death.

Cell cycle analysis

H2009 cells were harvested and pelleted after 72 h following siRNA transfection. Ice cold 70% ethanol was added to the pellet with mild vortexing to fix the cells. The fixed cells were kept at 4°C for PI staining. FxCycle™ PI/RNase Staining solution from Invitrogen was used for staining the DNA according to the manufacturer's protocol prior

the FACS analysis. Univariate model of Watson (Pragmatic) was used for cell cycle analysis.

Confocal microscopy

3D spheroids were seeded and imaged in 96-well clear ultra-low attachment microplates (Corning) using Zeiss LSM 880 confocal microscope with Airyscan at the Light Microscopy/Digital Imaging Core Facility at City of Hope. Images were processed using ZEN software and analyzed using ImageJ (Schneider et al, 2012).

Co-immunoprecipitation (Co-IP)

For all co-IP experiments, cells were lysed in the Pierce™ IP Lysis Buffer (Thermo Fisher Scientific) and 1 mg of protein was allowed to bind overnight in 4°C to agarose-conjugated antibodies (Santa Cruz Biotechnology): ITGB4 (Cat #: sc-13543 AC), FAK (Cat #: sc-271195 AC), PXN (Cat #: sc-365379 AC). IP beads were washed 5 times with 1X RIPA buffer and denatured in 2X reducing sample buffer at 95°C for 5 min. Western blots according to aforementioned protocol were performed to determine IP results. Multiple gels were run using the same lysates to detect all the specific antibodies. Exogeneous expression of ITGB4 and PXN was achieved in HEK293 cells by transfecting 7 ug of both pRK5 beta 4 and pBMN-PXN-HA-IRES-Hygro with Lipofectamine 3000 (Invitrogen) in a 10 cm dish. pRK5 beta4 was a gift from Filippo Giancotti (Dans et al, 2001) (Addgene plasmid # 16037; http://n2t.net/addgene:16037; RRID: Addgene16037). Cells were lysed 72h post transfection and co-IP was performed according to above protocol.

Proximity ligation assay (PLA)

To perform a complete Duolink® PLA *in situ* experiment, we used two primary antibodies (PLA, Immunofluorescence validated) that recognize PXN, ITGB4 or FAK epitopes. The starter kit from SIGMA supplies all other necessary reagents for Duolink® PLA reactions, which include a pair of PLA probes (Anti-Rabbit PLUS and Anti-Mouse MINUS), red detection reagents, wash buffers, and mounting medium. The primary antibodies used came from the same species as the Duolink® PLA probes for ITGB4 (Cell Signaling Technology, cat #: 4707)/PXN or FAK (Cell Signaling Technology, cat #: 3285) /PXN (clone 5H11, Invitrogen, cat #: MA5-13356) PLA. Analysis was carried out using standard immunofluorescence assay technique. We used a confocal microscope (LSM880) to capture images.

Seahorse XF Cell Mito Stress Test metabolic assay

Cells were seeded in complete growth medium on a Seahorse XF Cell Culture Microplate (Agilent Technologies, Santa Clara, CA, USA) to reach 90% monolayer confluence by the next day. One day prior to assay, 5 μM cisplatin was added for 24 h. On the day of the assay, mitochondrial inhibitor compounds were added to injection ports of the XFe96 FluxPak sensor cartridge at a final concentration of: oligomycin 1 μM, FCCP 1 μM, rotenone/antimycin A 1 μM each. Culture medium was changed to assay medium:

Seahorse XF RPMI medium supplemented with 1 mM sodium pyruvate, 2 mM L-glutamine, and 10 mM glucose. After completion of assay, cells were immediately stained with Hoechst dye and imaged using BioTek. Images were analyzed with QuPath (Bankhead et al, 2017) to obtain number of cells in each well and normalize data according to cell number.

ROS production assay

Cells were seeded in a 96-well plate and placed in an incubator at 37°C for 72 h. 50 µl of medium from each well was transferred to another 96-well plate to measure ROS production with ROS-Glo™ H_2O_2 Assay (Promega, Madison, WI, USA). Remaining cells on the first plate were used to perform CellTiter-Glo® Luminescent Cell Viability Assay (Promega) to normalize ROS data to number of viable cells. Luminescence was measured using a Tecan Spark 10M multimode microplate reader.

γH2AX foci staining and analysis

Cells were seeded (50,000 cells/well) on glass cover slips coated with 0.1% gelatin (Millipore) in a 12-well plate. Next day, 5 µM cisplatin was added for 24 h. Cells were fixed in 4% formaldehyde for 30 min at room temperature and blocked. Primary antibody against γH2AX (Cell Signaling Technology) was incubated in 4°C overnight. Then secondary antibody was incubated for 2 hours at room temperature. Cover slips were mounted on glass slides and imaged with Zeiss LSM 880 confocal microscope at the Light Microscopy/Digital Imaging Core Facility at City of Hope. Using QuPath (Bankhead et al, 2017), green fluorescent subcellular particles were counted in each nucleus to obtain γH2AX foci count per cell.

Chromatin immunoprecipitation (ChIP)

Briefly, five million formaldehyde-fixed cells were lysed in 200 µl of SDS lysis buffer and diluted to 2 ml in ChIP dilution buffer in the presence of protease inhibitors. Lysates were sonicated using Bioruptor PICO for 3 cycles and each cycle has 10 repeats of 30 sec pulse and 30 sec break. Lysates were precleared in salmon sperm DNA and protein A agarose by centrifugation. Prior to addition of antibody, 10% of the lysate was used for input and the remaining lysate was divided into two equal parts, one for IgG control and other for H3K27 acetylated antibody from Diagenode. Downstream processing of the chromatin bound antibody was done as per the manufacturer's protocol for EZ-magna ChIP A/G (Millipore, Temecula, CA). The extracted DNA was used for SYBR green based qPCR assay using the primers sequences Upstream USP1R-5'-AGGTTCACAGCATTCTCAATCC-3',UpstreamUSP1F-CAGTGCCTGTGAAACTTTGGA, Promoter USP1F-CTCAGCTCTACAGCATTCGC and Promoter USP1R-GGCCATCCAATGAGACAAGG. The data was analyzed based on the percentage of input.

Fluorescence-activated cell sorting (FACS) and analysis

Cells were trypsinized and resuspended (5 million) in PBS with 2% FBS. Cells were stained with ITGB4 antibody conjugated to Alexa Fluor® 488 (5 µl/1 million cells) (R&D Systems, Minneapolis, MN, USA) and Propidium Iodide Ready Flow™ Reagent (1 drop/1 million cells) (Invitrogen) for 30 min at 4°C. The Analytical Cytometry Core Facility at City of Hope carried out and assisted all FACS sorting and analysis experiments. Gates were set to sort cell populations having low 10% and high 10% expression of ITGB4 using the FACSAria™ Fusion (BD Biosciences, San Jose, CA, USA). Sorted cells were immediately cultured in 12-well plates and treated with cisplatin (1 µM) for 48 h. Then, equal number of untreated and treated cells were collected and stained with same reagents as above. FACS analysis was performed to determine shifts in cell population using the Attune NxT Flow Cytometer (Invitrogen).

Mathematical modeling

Bifurcation diagram was obtained using MATCONT (Dhooge et al, 2003). Next, Random circuit perturbation (RACIPE) algorithm was run on the two-node network – ITGB4/ miR-1-3p. The continuous gene expression levels were obtained as output with randomly chosen parameters for the regulatory links. The algorithm was used to generate 100,000 mathematical models, each with a different set of parameters for the following ODEs:

$$u = G_u H^s\left(I,\ I^0{}_u, n_{Iu},\ \lambda^-{}_{Iu}\right) - k_u u$$
$$I = G_I H^s\left(u,\ u^0{}_I, n_{uI},\ \lambda^-{}_{uI}\right) - k_I I$$

where, u denotes miR-1-3p and I denotes ITGB4. G_u and G_I are the maximum production rates of miR-1-3p and ITGB4 respectively. And, k_u and k_I are their innate degradation rates respectively.

Equations:

$$\mu^* = g_{\mu_{3p}} H^s\left(I,\ \lambda_{I,\mu_{3p}}\right) - m_I Y_\mu\left(\mu_{3p}\right) - k_{\mu_{3p}}\mu_{3p}$$
$$m_I{}^* = g_{mI} H^s\left(C,\ \lambda_{c,mI}\right) - m_I Y_m\left(\mu_{3p}\right) - k_{mI} m_I$$
$$I^* = g_I m_I L\left(\mu_{3p}\right) - k_I I$$

where H^S is the shifted Hill function, defined as $H^S\left(B,\lambda\right) = H^-\left(B\right) + \lambda H^+\left(B\right)$,

$H^-\left(B\right) = 1/\left[1+\left(B\ /\ B_0\right)^{nB}\right]$, $H^+\left(B\right) = 1 - H^-\left(B\right)$ and λ is the fold change from the basal synthesis rate due to protein B. λ >1 for activators, while λ <1 for inhibitors.

The total translation rate:

$$m_I L(\mu_{3p}) = m\sum_{(i=0)}^{n} l_i C_n^i M_n^i(\mu)$$

The total mRNA active degradation rate:

$$m_I Y_m\left(\mu_{3p}\right) = m\sum_{(i=0)}^{n} \gamma_{m_i} C_n^i M_n^i(\mu)$$

The total miR active degradation rate is

$$m_I Y_\mu\left(\mu_{3p}\right) = m\sum_{(i=0)}^{n} \gamma_{\mu_i} C_n^i M_n^i(\mu)$$

Parameters used in panel A:

n (# of miR binding sites)		0	1	2	3
L only	l_i	1.0	0.5	0.2	0.02
Y only	γ_{mi} (Hour^{-1})		0.3	1.5	7.5
Both, L stronger	l_i	1.0	0.6	0.3	0.1
	γ_{mi} (Hour^{-1})		0.04	0.2	1.0
----	γ_{mi} (Hour^{-1})		0.005	0.05	0.5

Parameter	**Value**
$k_{\mu 3p}$ (hour^{-1})	0.05
k_{mI} (hour^{-1})	0.5
k_I (hour^{-1})	0.1
$g_{\mu 3p}$ (molecules/hour)	2900
g_{mI} (molecules/hour)	30
g_I (hour^{-1})	100

$I^0_{\mu 3p}$ **(molecules)**	6000
$\mu 3p^0$ **(molecules)**	10000
C^0_{ml} **(molecules)**	250000
$n_{I,\mu 3p}$	3
$n_{\mu 3p}$	6
$n_{C,ml}$	3
$\lambda_{I,\mu 3p}$	0.3
$\lambda_{C,ml}$	10

The feedback loop was constructed based on data reported in the manuscript (ITGB4 inhibits miR-1-3p) and publicly available data (miR-1-3p inhibits ITGB4) - https://www.genecards.org/cgi-bin/carddisp.pl?gene=ITGB4.

The parameters for microRNA-mediated dynamics were estimated from our previous models for microRNA-mediated regulation of EMT (Lu et al. 2013).

Supplemental References

Bankhead, P., Loughrey M. B., Fernández, J. A., et al. (2017). QuPath: Open source software for digital pathology image analysis. Sci Rep. *7*, 16878.

Dans, M., Gagnoux-Palacios, L., Blaikie, P., Klein, S., Mariotti, A., and Giancotti, F. G. (2001). Tyrosine phosphorylation of the beta 4 integrin cytoplasmic domain mediates Shc signaling to extracellular signal-regulated kinase and antagonizes formation of hemidesmosomes. J Biol Chem. *276*, 1494-1502.

Dhooge, A., Govaerts, W., and Kuznetsov, Y. A. (2003). MATCONT: A Matlab package for numerical bifurcation analysis of ODEs. ACM Transactions on Mathematical Software *29*, 141–164.

Lu, M., Jolly, M.K., Levine, H., Onuchic, J.N., Ben-Jacob, E. (2013). MicroRNA-based regulation of epithelial-hybrid-mesenchymal fate determination. Proc Natl Acad Sci U S A ***110***, 18144–18149.

Schneider, C. A., Rasband, W. S., and Eliceiri, K. W. (2012). NIH Image to ImageJ: 25 years of image analysis. Nat Methods *9*, 671-675.